

K* x-ray emission from 20- to 36-MeV fluorine projectiles following electron capture to excited states

M. D. Brown, L. D. Ellsworth, J. A. Guffey, T. Chiao,[†]
E. W. Pettus,[‡] L. M. Winters, and J. R. Macdonald

Department of Physics and Nuclear Science Laboratory, Kansas State University, Manhattan, Kansas 66506

(Received 13 May 1974)

The projectile *K* x-ray emission cross sections for fluorine ions were measured under single collision conditions for charge states ranging from +4 to +9 in a thin argon target. The dependence of these cross sections upon the energy and the initial charge state of the projectile was determined for fluorine ions with energies between 20 and 36 MeV. Over the entire energy range, the *K* x-ray-production cross section for F^{+9} ions was about 70% of the total electron-capture cross section determined in a separate experiment. The *K* x-ray-production cross section for these fully stripped ions is attributed to electron capture to excited states of the projectile. Calculations of electron-capture cross sections within the Brinkman-Kramers approximation for these heavy-ion collisions are consistent with the observation of large cross sections for capture to excited states.

I. INTRODUCTION

When highly stripped, swift, heavy ions interact with matter, multiple ionization and excitation commonly occur in both the projectile and the target atom. For the projectile, electron capture and loss¹ is a major feature of these fast heavy-ion collisions. Electron transfer to highly excited states of fast proton beams has been studied in some detail.² For fast heavy ions, electron capture to excited states in the projectile³ may dominate the capture cross section. In this paper we report observations of the fluorine *K* x rays emitted after collisions with argon atoms and measurements of the projectile x-ray-production cross sections. For the bare (F^{+9}) projectile, the *K* x rays observed are radiative decays which only occur following electron capture to excited states of the projectile; while in the more complicated case for the one-electron (F^{+8}) beam, this electron capture dominates excitation processes in the production of *K* x rays. The experimental F^{+8} and F^{+9} x-ray-production cross sections were compared to predictions for electron capture calculated in a Brinkman-Kramers⁴ approximation. For this comparison the calculations were normalized to the total experimental electron-capture cross sections.⁵ Excellent agreement was found between both the F^{+9} and F^{+8} x-ray-production cross sections and the predicted cross section for capture to excited states. From the experiment with the bare nucleus, the *K* x-ray production is about 70% of the total capture cross section while for the calculated results excited-state capture is about 90% of the total.

In this velocity range, electron-capture cross

sections are larger than ionization cross sections, hence, the *K* x-ray yield from the projectile is very sensitive to the charge q of the incident ion. Since electron capture to excited states will not produce *K* x rays in projectiles with a filled *K* shell, a large decrease in cross section is expected for F^{+7} as compared to F^{+8} ions. The dependence of the fluorine *K* x-ray cross sections upon the incident projectile charge state was determined for charge states ranging from +4 to +9 in this experiment. At 20.3 MeV the fluorine *K* x-ray-production cross section increases 40-fold as the projectile charge increases from +4 to +9 as compared to a sevenfold increase at 35.6 MeV. The dependence of the x-ray yields upon the incident charge state may be understood by considering the relative importance of electron capture, fluorescence yield, inner-shell ionization, and excitation. For projectiles with two or more electrons inner-shell ionization and excitation of electrons in the projectile produce the *K* x rays. Both of these processes are expected to increase with projectile energy in the region studied and a corresponding increase in the x-ray yields is observed. By contrast, the cross section for capture of electrons to excited states of the F^{+9} and F^{+8} ions monotonically decreases with increasing projectile energy and a corresponding decrease in the x-ray yields is observed. The large capture cross section for F^{+9} and the small *K*-vacancy-production cross section and associated fluorescence yield for the few electron ions are responsible for the projectile-charge-state dependence and its variation with projectile energy.

Recent experiments have shown that the target x-ray production is dependent on the projectile

charge state for fast collisions of heavy ions with both gas⁶⁻¹² and solid¹³ targets. A greater than Z_1^2 dependence of argon *K*-shell vacancy production upon the nuclear charge Z_1 of the projectile has been reported¹⁴ for fully stripped projectiles of F, O, N, and C with energies ranging from 1 to 2 MeV/amu. Existing theories^{15,16} of inner-shell Coulomb ionization assume the projectile is a structureless point charge and, if extrapolated to these collisions, would predict that the inner-shell vacancy production in the target is quadratic in the projectile nuclear charge for different nuclei incident on the same target at the same velocity. It has been suggested recently that electron capture to bound states of the projectile contributes significantly to the vacancy production^{17,18} and should be included in addition to the Coulomb ionization. Reasonable relative agreement with the experimental measurements for bare nuclei has been shown. However, no existing theory is able to produce the strong dependence of the target x-ray yield upon the ionic charge state of the projectile.

Compared to the charge dependence of the target x-ray production, the *K* x-ray yield from the projectile exhibits an even stronger dependence upon the ionic charge state. In addition, the x-ray yield is very sensitive to the atomic number Z_2 of the target.^{19,20} For a neon-gas target, the neon *K* x-ray yield increased 60-fold while the projectile *K* x-ray yield increased more than 1000-fold when the charge state of an ≈ 80 -MeV argon beam was increased from +6 to +17.⁸ It may be the large cross sections for electron transfer from neon to excited states in argon which are responsible for the large increase in the argon *K* x-ray yield. The existence of these charge-dependent effects is clearly important in any interpretation of x rays produced in fast heavy-ion collisions. For solid targets and thick gas cells where charge changing may be considerable in multiple collisions, care must be taken in any determination of x-ray yields.

II. EXPERIMENTAL APPARATUS AND METHODS

Fluorine-ion beams were accelerated by the tandem Van de Graaff Accelerator at Kansas State University and momentum analyzed by a 90° bending magnet. Fluorine-ion beams with energies 20.3, 30.0, and 35.6 MeV [corresponding to velocities $(1.4, 1.7, \text{ and } 1.9) \times 10^9$ cm/sec] were separated into charge states from +4 to +9 by passing the beam through a thin carbon foil which produced an equilibrium charge-state distribution in the beam. A particular charge state was selected from the beam using a switching magnet which directed the beam to the differentially

pumped gas cell. The gas cell¹⁰ was defined by four apertures with diameters, 1, 1.5, 2.5, and 3 mm arranged in increasing size as the beam passed through the cell. Two 6-in diffusion pumps evacuated the regions just before and just after the gas cell. The charge-state purity of the incident beam was always greater than 99% with only residual gas ($\approx 5 \times 10^{-5}$ Torr) in the cell. The gas-target thicknesses used were such that less than 5% of the incident beam suffered charge-changing collisions in the gas cell. The prerequisite was used to ensure single-collision conditions for charge exchange. The beam current was measured in three Faraday cups that were suppressed with -500 V and located between the first and second apertures, the second and third apertures and directly behind the fourth aperture. The beam transmission through the gas cell was monitored and maintained at 100% using these cups. Beam currents of a few nA were typical for each charge state. The particle intensity was determined from the beam integrated in the final Faraday cup using a current digitizer.

Two experimental arrangements were used to obtain the data. In the first, the fluorine *K* x rays produced in the argon-gas target were detected in a flow-mode proportional counter with a 2.0- μ m foil window²¹ while a Si(Li) detector simultaneously monitored the argon *K* x rays. Carbon sleeves mounted about the two inner apertures and defining the 3.5-cm interaction region shielded the apertures themselves from the view of both detectors. In this manner any stray beam which might strike an aperture was not seen by either detector. The fluorine *K* x-ray-production cross section was then determined by normalizing the fluorine x rays counted in the proportional counter to the argon *K* x rays detected in the Si(Li) detector and the previously measured¹⁰ argon *K* x-ray cross sections. This normalization made beam current and target-pressure measurements unnecessary. In the second arrangement, absolute measurements were made using a calibrated capacitance manometer coupled with a servo-mechanical valve maintaining the gas target at a known pressure ranging from 1 to 10 mTorr. As expected, a linear growth of x-ray yield with target pressure was observed for each charge state. A typical growth curve is shown in Fig. 1. This linear growth is evidence that we were in the pressure region for single-collision events. During these second measurements, the window of the proportional counter was found to leak gas (90% argon, 10% methane) into the argon-gas target. This caused a slight offset in the zero pressure (≈ 1 mTorr) and introduced a contaminant gas that produced a negligible systematic error

in the final cross sections taken from the growth curve. The product of solid angle and interaction length (the total geometrical factor used to determine cross sections from x-ray yields) was obtained by integrating the detector solid angle over the interaction length it viewed. This value for the proportional counter was varied from 1.36×10^{-2} to 1.75×10^{-3} cm and found to be calculable from the defining dimensions.

The largest source of error in these measurements is uncertainty in the transmission through the proportional-counter window and, hence, detector efficiency. The Si(Li) detector counts fluorine *K* x rays, but its detection efficiency of about 1% is strongly energy dependent and is much too poorly known to make accurate cross-section measurements. The necessary window-transmission correction for the proportional counter was deduced using the quantum efficiency curve supplied by the manufacturer²¹ and the distribution and relative intensities of the lines as observed in high-resolution measurements²² for F^{+9} and F^{+8} . This correction was determined by weighting the efficiency for each spectral component by its relative intensity. In this manner effective detector efficiencies of 38% and 30% were derived for F^{+9} and F^{+8} beams, respectively. The detector has an efficiency of 16.5% for the 677-eV $K\alpha$ x ray of atomic fluorine. The detector efficiency was estimated by interpolation to be 25% for F^{+7} , 22% for F^{+5} , and 19% for F^{+4} . This detection efficiency, which is known to depend on the energy distribution of the fluorine *K* x-ray lines, was assumed to be independent of the beam energy over the region studied. The estimated uncertainty in this detection efficiency varies from $\pm 10\%$ for F^{+9} and F^{+8} to $\pm 20\%$ for the rest. Any correction for thickness variation or impurity

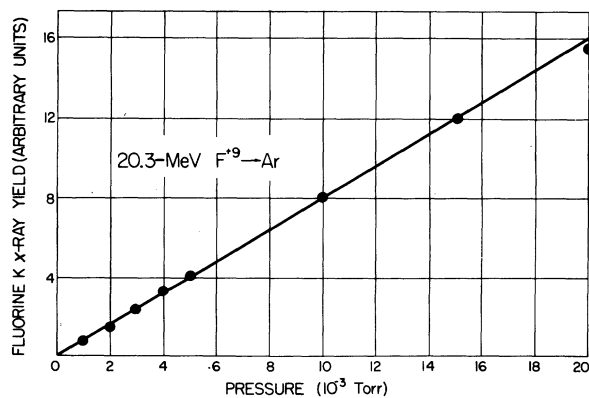


FIG. 1. Fluorine *K* x-ray yield vs target pressure for 20.3-MeV F^{+9} bombarding argon. The yields are normalized to a constant value of charge collected in the final Faraday cup.

content in the foil window has been ignored. The capacitance manometer has an uncertainty in its calibration of $\pm 10\%$, and the total geometrical factor is estimated to have a $\pm 15\%$ uncertainty. The x-ray-production cross sections are estimated to have a total uncertainty of $\pm 30\%$ taking into account all errors. The relative error between the cross sections for different charge states and various energies is somewhat smaller ($\approx 10\%$), since most of the uncertainties are systematic in nature.

III. ELECTRON-CAPTURE CALCULATIONS

Since fluorine *K* x rays can be produced by bare fluorine nuclei only following electron capture in collisions with argon, we have used the simple generalization of the Brinkman-Kramers formulation by Nikolaev to compare theory and experiment. This formulation [see Eq. (10) in Ref. 3] allows one to estimate the relative importance of electron capture from the various shells of the target atom to each hydrogenic state of the projectile. However, it does not permit identification of the orbital quantum number or the magnetic quantum number in either the target or the projectile. The results of this calculation²³ for the electron capture by 20-MeV F^{+9} ions bombarding argon, given in Fig. 2, show that the largest cross

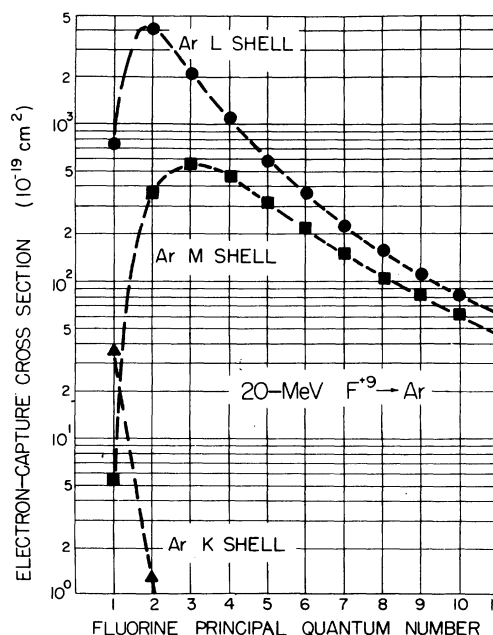


FIG. 2. Cross sections for electron transfer from the *K*, *L*, or *M* shell of the target argon atom to states with principal quantum number *n* in the fluorine projectile. The cross sections for 20-MeV F^{+9} ions bombarding argon were calculated using Eq. (10) in Ref. 3.

section occurs for electron transfer from the L shell of argon to the $n=2$ state of hydrogenic fluorine. This cross section corresponds to the case when the binding energy of the electron in the target atom is approximately equal to the binding energy of the electron in the projectile. The binding energies are $E_K \approx 3210$ eV, $E_L \approx 270$ eV, and $E_M \approx 20$ eV for the K , L , and M shells of argon, respectively, and the binding energy in hydrogenlike fluorine is 1100 eV for $n=1$, 275 eV for $n=2$, and 122 eV for $n=3$. In the case of 20-MeV F^{+9} on argon, the calculation gives 94% of the electron capture to excited states ($n \geq 2$) of the projectile with 38% to the $n=2$ level of fluorine, 22% to the $n=3$ level, and 13% to the $n=4$ level. These large cross sections for electron transfer into excited states of the projectile are responsible for the large ($>10^{-17}$ cm²) cross sections for fluorine K x-ray production observed in this experiment.

It is well known that the Brinkman-Kramers approximation overestimates (≈ 3 times) the cross sections for electron capture by protons.³ However, the energy dependence is nearly correct. For the fluorine beams the electron-capture cross section is overestimated by an even greater amount (≈ 10 – 20 times) while its energy dependence is also nearly correct. In order to use the Brinkman-Kramers formulation to make comparisons with experimental measurements, all calculated total electron-capture cross sections were normalized to the total experimental cross sections for electron capture. In Table I are listed the experimentally measured electron-capture cross sections⁵ for fluorine ions with energies of 20, 30, and 36 MeV and the calculated unnormalized total electron-capture cross sections for F^{+9} and F^{+8} bombarding argon. The calculations²³ are only for single-electron capture whereas we should point out that 18% of the total experimental electron capture is double capture⁵ for 20-MeV F^{+9} ions.

After normalization, this Brinkman-Kramers approximation may be used to estimate the relative role of electron capture to each final state in the projectile. In the calculation the F^{+8} is assumed to be unscreened ($q=8$) and hydrogenic whereas the capture is to heliumlike states. This formulation can also estimate the relative importance of electron capture from individual shells of the target. This will be discussed in Sec. IV.

IV. RESULTS AND DISCUSSION

We have measured the K x-ray cross sections for fluorine ions with energies of 20.3, 30.0, and 35.6 MeV and for several initial projectile charge states. These cross sections are displayed in Fig. 3 as a function of fluorine-ion energy. The cross section for the F^{+9} bare nuclei, which monotonically decreases with increasing energy, must arise from electron capture to excited states of the fluorine projectile. Because of the energy dependence of the cross section for the F^{+8} beam, we conclude that electron capture to excited states is the dominant mechanism rather than excitation of the single fluorine electron or some multiple process. For the F^{+7} beam the K shell contains both electrons so only excitation of the bound electrons or some multiple process can account for the observed K x rays. All lower charge states produce x rays by K -shell ionization of the projectile, excitation, or multiple processes which produce K vacancies in the fluorine ion. In this velocity region Coulomb ionization and excitation are monotonically increasing with increasing projectile energy.¹⁵

Since the fluorine K x rays produced when F^{+9} bombards argon must follow electron capture to excited states of the fluorine projectile, we can compare the experimental measurements with the predictions for electron capture. The cross sections for electron capture into excited states for both F^{+8} and F^{+9} ions were calculated using Eq.

TABLE I. Single (σ_1), double (σ_2), triple (σ_3), and total experimental [σ_T (expt.)] electron-capture cross sections taken from Ref. 5 and total [σ_T (calc.)] electron-capture cross sections calculated from Ref. 3. The cross sections are for the fluorine ions with incident charge state q , bombarding argon with energies of 20, 30, and 36 MeV.

	Electron-capture cross sections (10^{-18} cm ²)											
	20-MeV F^{+q} on argon				30-MeV F^{+q} on argon				36-MeV F^{+q} on argon			
	$q=6$	$q=7$	$q=8$	$q=9$	$q=6$	$q=7$	$q=8$	$q=9$	$q=6$	$q=7$	$q=8$	$q=9$
σ_1	17	27	45	52	7	14	27	33	4	7	18	25
σ_2	1	3	5	12	0.2	0.8	2	5	0.1	0.3	1	4
σ_3	...	0.2	0.8	2	0.3	1	0.4
σ_T (expt.)	18	30	51	66	7	14	29	39	4	7	19	29
σ_T (calc.)			850	1200			320	440			200	280

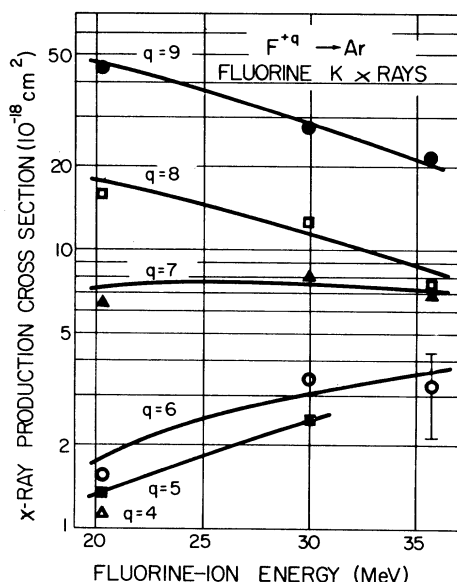


FIG. 3. Experimental fluorine K x-ray-production cross sections vs fluorine-ion energy for several incident charge states.

(10) in Ref. 3 after normalizing the calculation so that the total cross section calculated at each energy was equal to the total experimental electron capture observed⁵ at that same energy. These cross sections for electron capture into excited states for both F^{+8} and F^{+9} ions are listed in Table II with the experimental x-ray-production cross sections. Since the electron capture may be to states which are long lived and do not decay within the field of view of the detector, only a fraction of the excited-state capture will result in x rays observed in this experiment. Since an understanding of this fraction is complicated by the distribution of the resulting branching ratios, a best fit (81% for F^{+9} , 49% for F^{+8}) to the experimental measurements was chosen. The calculated cross sections for electron capture, after normalization and modification by these fractions,

TABLE II. Experimentally determined fluorine K x-ray-production cross sections (σ_x) for F^{+8} and F^{+9} ions with energies of 20.3-, 30.0-, and 35.6-MeV bombarding argon and the normalized cross section for electron capture to excited states [$\sigma_c (n \geq 2)$] calculated from Eq. (10) in Ref. 3 for F^{+8} and F^{+9} beams, respectively.

Energy (MeV)	Cross sections (10^{-17} cm^2)			
	$\sigma_c (n \geq 2)$	σ_x	$\sigma_c (n \geq 2)$	σ_x
20.3	6.1	4.6	4.3	1.6
30.0	3.4	2.7	2.2	1.3
35.6	2.4	2.2	1.4	0.76

are shown in Fig. 4 with the corresponding experimental x-ray-production cross sections. Clearly the agreement is excellent.

There are several long-lived states which are formed in these collisions that may account for the fraction of states decaying radiatively. High- n states ($n > 11$) have a long lifetime and would not yield observable K x rays for F^{+8} and F^{+9} . In the case of the $n=2$ level of hydrogenlike fluorine only the $2s$ state is metastable. If, for example, a statistical weighting of the electronic spin states occurs in the electron-capture process, then only 75% of the electron capture to the $n=2$ level produces an observed x ray. There are two $^2S_{1/2}$ substates, two $^2P_{1/2}$ substates, and four $^2P_{3/2}$ substates for a total of eight. The decay from $^2S_{1/2}$ which has a lifetime²⁴ of 230 nsec, is forbidden; whereas, both the $^2P_{1/2}$ and $^2P_{3/2}$ have allowed electric dipole transitions to the ground state. Clearly the 81% of the electron capture to excited states chosen to best fit the experimental measurements shown in Fig. 4 is a quite reasonable fraction of capture which produces observed x rays. In a similar manner the $n=2$ level of heliumlike fluorine produces prompt K x rays only 37.5% of the time. In this example, for two-electron fluorine, there are three 3S_1 , one 1S_0 , five 3P_2 , and one 3P_0 for a total of ten substates which are metastable²⁴ and, hence, do not decay

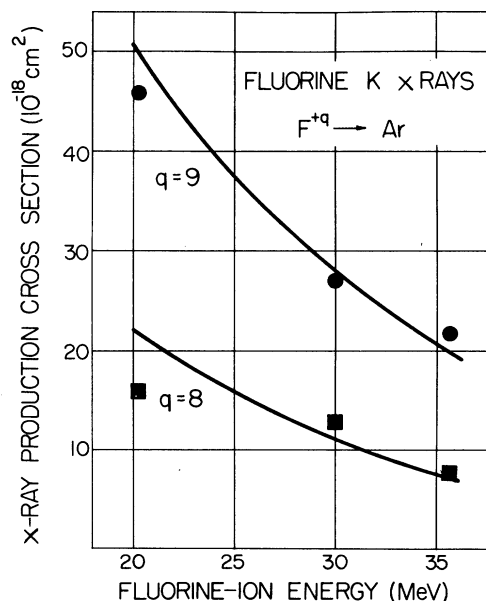


FIG. 4. Experimental fluorine K x-ray-production cross sections for both F^{+8} and F^{+9} ions as a function of fluorine-ion energy. Solid lines, 81% of the normalized cross section for electron capture to excited states for F^{+9} ions and 49% of the normalized cross section for F^{+8} ions.

while within view of the detector. The three 3P_1 and three 1P_1 substates do yield observable K x rays when formed. A total of six out of 16 substates yield observable K x rays, and this is a reasonable match with the 49% of the capture to excited states which best fits the measurements for F^{+8} . We point out that the F^{+8} beam can also produce K x rays by excitation, but this process has the wrong projectile energy dependence since both excitation and ionization should be monotonically rising with increasing fluorine energy over this energy interval.

For the lower charge states the expected uniform rise of the excitation and ionization cross sections with increasing projectile energy explains the increase of the K x-ray-production cross section with fluorine energy for incident charge states +5 and +6 as shown in Fig. 3. For these charge states care must be taken to account properly for the effective fluorescence yields if some knowledge of the K -shell vacancy production is desired. With the present imperfect knowledge of the fluorescence yield, we have not attempted to derive vacancy-production cross sections. Figure 5 displays the fluorine K x-ray-production cross section as a function of incident charge state for 20.3-MeV fluorine on argon. The cross section increases 40-fold as the incident charge state increases from +4 to +9. This 40-fold increase arises from the large capture cross section for F^{+9} which gives a high yield and the small ionization and excitation coupled with a small fluorescence yield which gives a low yield for the lower

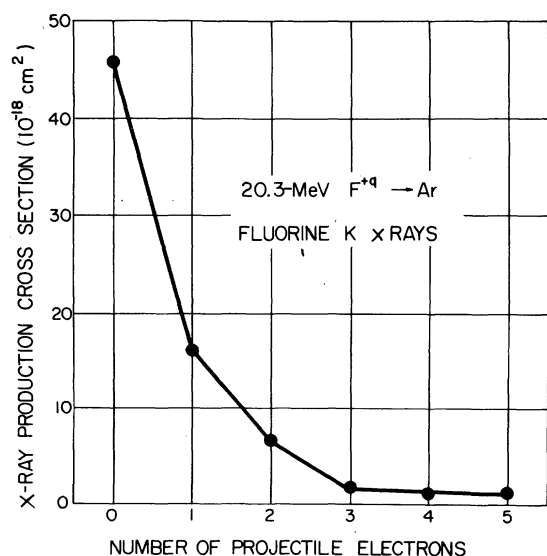


FIG. 5. Fluorine K x-ray-production cross sections for 20.3-MeV fluorine ions bombarding argon vs the incident projectile charge state.

charge states. Clearly, this large dependence of projectile x-ray production upon incident charge state places severe limitations on the interpretation of projectile x rays produced in solid targets where the equilibrium charge-state distribution of the beam must somehow be taken into account.

In these same collisions argon K x rays are produced. Recently, it has been suggested^{17,18} that the K -shell vacancy production in argon results from the two processes of inner-shell ionization and electron capture by the projectile from the argon K shell. One can examine this suggestion for the F^{+8} and F^{+9} collisions. The inner-shell ionization cross section may be taken as Z_1^2 times the measured ionization cross section produced by protons with the same velocity. The cross section for electron capture from the K shell of argon was found using Eq. (10) in Ref. 3 after normalizing the total calculated cross section as before. In Table III the experimental cross sections for inner-shell ionization of argon by F^{+8} and F^{+9} ions, the normalized cross section for electron capture from the K shell of argon for both F^{+8} and F^{+9} ions, and 81 times the ionization cross section for protons on argon^{10,25} are listed for beam energies of 20, 30, and 35.5 MeV. The energy dependence for both electron capture and direct ionization compare reasonably with the experimental results; however, the sum of the direct ionization and electron-capture cross sections exceeds the measured vacancy-production cross sections. In fact, electron capture alone can nearly account for the measured cross sections. A comparison of the measured argon K -vacancy-production cross section with the predictions of electron capture is shown in Fig. 6. Although only a small fraction of the total capture (0.3% by 20-MeV F^{+9}) is from the K shell of argon, it can account for both the magnitude and the ener-

TABLE III. Scaled argon K -shell ionization cross section ($Z_1^2\sigma_I$) for protons from Ref. 10, the experimental cross sections for argon K -shell vacancy production (σ_v) by F^{+8} and F^{+9} also from Ref. 10, and the normalized cross section for electron capture (σ_c) from the K shell of argon for 20-, 30-, and 35.5-MeV beams of F^{+8} and F^{+9} ions calculated from Eq. (10) in Ref. 3.

Energy (MeV)	Cross sections (10^{-20} cm^2)				
	$81\sigma_I$	σ_c	σ_v	σ_c	σ_v
20	9	21	23.1	9	10.0
30	17	44	50.9	20	26.0
35.5	22	52	61.1	23	34.0

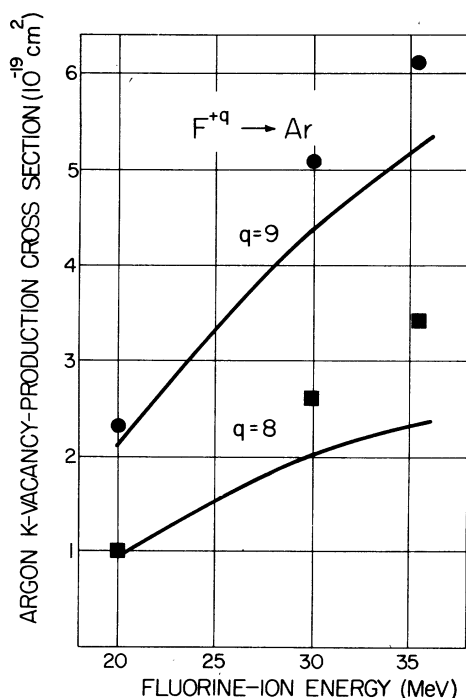


FIG. 6. Experimental argon K -shell vacancy-production cross section taken from Ref. 10 plotted against fluorine-ion energy for F^{+8} and F^{+9} beams. Solid lines, normalized calculations for electron capture from the K shell of argon.

gy dependence of the argon K -vacancy production. The agreement of these calculations with the measurements indicates that electron capture has a dominant role in the production of K x rays from

both the target and the projectile for F^{+9} and F^{+8} ion beams.

V. SUMMARY AND CONCLUSIONS

We have observed the incident charge-state dependence of fluorine K x-ray production in collisions of 20- to 36-MeV fluorine beams with argon. We show that normalization of a total Brinkman-Kramers electron-capture cross section to the total measured capture cross section can predict the observed argon K x-ray production and the fluorine K x-ray production for both bare and one-electron fluorine projectiles. The predictions of this formulation are too large in absolute magnitude but nearly correct in their projectile energy dependence. These predictions may have the correct dependence on both projectile and target principal quantum number and projectile charge state. A large (40-fold) dependence of fluorine K x-ray production upon incident charge state is observed to decrease with projectile energy. We conclude that electron capture, and particularly electron capture to excited states of the projectile, is important in these fast heavy-ion collisions.

ACKNOWLEDGMENT

The authors are grateful to Dr. James H. McGuire for many valuable remarks during discussions of the present work.

*Work partially supported by the U. S. Atomic Energy Commission under Contract No. AT(11-1)-2130.

†Present address: Cyclotron Institute, Texas A & M University, College Station, Tex. 77843.

‡Present address: National Accelerator Laboratory, P. O. Box 500, Batavia, Ill. 60510.

¹Two review articles on electron capture and loss are V. S. Nikolaev, *Usp. Fiz. Nauk* **85**, 679 (1965) [*Sov. Phys.—USP.* **8**, 269 (1965)] and H. D. Betz, *Rev. Mod. Phys.* **44**, 465 (1972).

²See J. E. Bayfield, G. A. Khayrallah, and P. M. Kock, *Phys. Rev. A* **9**, 219 (1974) and references cited therein.

³V. S. Nikolaev, *Zh. Eksp. Teor. Fiz.* **51**, 1263 (1966) [*Sov. Phys.—JETP* **24**, 847 (1967)].

⁴H. C. Brinkman and H. A. Kramers, *Proc. Acad. Sci. Amsterdam* **33** 973 (1930).

⁵S. M. Ferguson, J. R. Macdonald, T. Chiao, L. D. Ellsworth, and S. A. Savoy, *Phys. Rev. A* **8**, 2417 (1973) and T. Chiao, Ph.D. thesis (Kansas State University, 1973) (unpublished).

⁶J. R. Macdonald, L. Winters, M. D. Brown, T. Chiao,

and L. D. Ellsworth, *Phys. Rev. Lett.* **29**, 1291 (1972).

⁷J. R. Mowat, D. J. Pegg, R. S. Peterson, P. M. Griffin, and I. A. Sellin, *Phys. Rev. Lett.* **29**, 1577 (1972).

⁸J. R. Mowat, I. A. Sellin, D. J. Pegg, R. S. Peterson, M. D. Brown, and J. R. Macdonald, *Phys. Rev. Lett.* **30**, 1289 (1973).

⁹R. L. Kauffman, F. Hopkins, C. W. Woods, and P. Richard, *Phys. Rev. Lett.* **31**, 621 (1973).

¹⁰L. M. Winters, J. R. Macdonald, M. D. Brown, T. Chiao, L. D. Ellsworth, and E. W. Pettus, *Phys. Rev. A* **4**, 1835 (1973).

¹¹M. D. Brown, J. R. Macdonald, P. Richard, J. R. Mowat, and I. A. Sellin, *Phys. Rev. A* **9**, 1470 (1974).

¹²J. R. Mowat, I. A. Sellin, P. M. Griffin, D. J. Pegg, and R. S. Peterson, *Phys. Rev. A* **9**, 644 (1974).

¹³W. Brandt, R. Laubert, M. Maurino, and A. Schwarzschild, *Phys. Rev. Lett.* **30**, 358 (1972).

¹⁴J. R. Macdonald, L. M. Winters, M. D. Brown, L. D. Ellsworth, T. Chiao, and E. W. Pettus, *Phys. Rev. Lett.* **30**, 251 (1973).

¹⁵E. Merzbacher and H. W. Lewis, in *Handbuch der Physik*, edited by S. Flügge (Springer, Berlin, 1958),

Vol. 34, p. 166.

- ¹⁶J. D. Garcia, Phys. Rev. A 1, 280 (1970); Phys. Rev. A 1, 1402 (1970).
- ¹⁷J. H. McGuire, Phys. Rev. A 8, 2760 (1973).
- ¹⁸A. M. Halpern and J. Law, Phys. Rev. Lett. 31, 4 (1973).
- ¹⁹L. Winters, J. R. Macdonald, M. D. Brown, T. Chiao, L. D. Ellsworth, and E. W. Pettus, Phys. Rev. Lett. 31, 1344 (1973).
- ²⁰H. Kubo, F. C. Jundt, and K. H. Purser, Phys. Rev. Lett. 31, 674 (1973).
- ²¹Siemens Corporation, Karlsruhe, Germany supplied both the proportional counter and foil windows.
- ²²J. R. Macdonald, P. Richard, C. L. Cocke, M. D. Brown, and I. A. Sellin, Phys. Rev. Lett. 31, 684 (1973).
- ²³For details of these calculations see J. A. Guffey, M.Sc. thesis (Kansas State University, 1974), and work to be published.
- ²⁴R. A. Marrus, Nucl. Instrum. Meth. 110, 333 (1973).
- ²⁵L. M. Winters, J. R. Macdonald, M. D. Brown, L. D. Ellsworth, and T. Chiao, Phys. Rev. A 7, 1276 (1973).